Viscoelastic Properties of Blends of Styrene–Butadiene Diblock Copolymer and Low Molecular Weight Homopolybutadiene

Hiroshi Watanabe and Tadao Kotaka*

Department of Macromolecular Science, Faculty of Science, Osaka University, Toyonaka, Osaka 560, Japan. *Received September 15, 1982*

ABSTRACT: Linear viscoelastic behavior of five well-characterized styrene–butadiene (SB) diblock copolymers blended with a low molecular weight homopolybutadiene (chB) was examined. Since chB is a nonsolvent for polystyrene, the S blocks precipitate to form spherical microdomains, and micelles with S cores and B cilia are formed in the blends. As long as the SB content is low, such a blend shows a Newtonian behavior in the region of low frequency. However, when the SB content exceeds a certain critical value, the blend exhibits a plateau in the low-frequency tails of the storage (G') and loss (G'') moduli. The plateau is often called a second plateau and is related to some slow relaxation process existing in the system. The critical concentration almost coincides with the concentration at which the micelles begin to contact and their cilia begin to overlap with each other. Nevertheless, the activation energy of flow for the SB/chB blends in any concentration is the same as that of the chB homopolymer. These results suggest that the slow relaxation mechanism is related to the motion of the entangled B blocks with one end anchored on the S core. The longest relaxation time τ_p for such slow relaxation process increases exponentially with increasing concentration. This exponential enhancement is typical to the relaxation of a polymer chain with a spatially fixed end, often employed as a model for the star-shaped polymers. From this viewpoint, the "tube" model of Doi and Edwards was employed for partially entangled B blocks with one end anchored on the S cores. The dependencies of τ_p for the five SB/chB blends on the concentration and molecular weight of SB could be reduced to a universal relation, which coincided with the theoretical results derived from the tube model.

I. Introduction

Solutions of styrene–butadiene (SB) diblock copolymers in selective solvents, which dissolve only one of the blocks but precipitate the other, often show peculiar rheology.[1-3] For example, solutions of an SB diblock copolymer in *n*-alkane, which dissolves only B blocks, often show plastic flow with thixotropy in steady flow measurements[1-3] and nonlinear *viscoelastoplasticity* in dynamic measurements.[4] Recently, we examined the plasticity of such solutions and found that it resulted from a "structure" formed in the systems,[4-7] in which micelles of S cores and B cilia are arranged on a regular three-dimensional simple cubic array, which we call the "macrolattice". The macrolattice structure in such a system is lost either by dilution or by heat. The system having no macrolattice does not show nonlinear plastic behavior but exhibits linear viscoelasticity.

In a previous paper,[5] we proposed an idea explaining the driving force of the macrolattice formation. The driving force is attributable to a spatial gradient of the concentration of the dissolved B blocks. Deformation of the macrolattice causes an additional increase in the concentration gradient and, therefore, increase in the free energy of the system. This driving force is similar in nature to the thermodynamic force determining the domain sizes and morphology[8,9] in bulk block copolymers. However, its magnitude is much smaller than that in the bulk where no change in density is allowed.

Our idea for the driving force of the macrolattice formation is supported by the following two experimental results: One is that the critical concentration, above which the macrolattice is formed and the solution exhibits plasticity, is well predicted from the size of the micelles;[10] the critical concentration is almost the same as the critical threshold where the long-range concentration gradient becomes strongly inhibited and the osmotic pressure strongly emerges. The second is that the micelle system loses its plasticity when a commercially available low molecular weight homopolybutadiene (chB) is added to the system,[11,12] instead of usual selective solvents such as *n*-alkanes. Both chB and *n*-alkanes precipitate S blocks but dissolve B blocks. However, in the chB solvent, the concentration change of B segments cannot be generated upon deformation because the chB molecules are chemically identical with the B blocks. The freely mobile chB molecules act as a buffer to suppress the concentration change and to break down the regular macrolattice.

Table I
Characteristics of Polymer Samples

code	$10^{-3}M_n$	M_w/M_n	PS cont/ wt %	$10^{-3}M_n$ of S block
SB1	66	1.06	29.3	20
SB2	117	1.07	16.1	20
SB3	134	1.07	24.0	32
SB4	192	1.08	17.0	32
SB5	294	1.10	11.0	32
chB[a]	2	2	0	0

[a] A commercially available sample, Nisseki liquid polybutadiene PB 2000.

As described above, in the blends of SB diblock copolymer and chB the change in the concentration of B segments is completely screened. Therefore, such blends do not possess plasticity but show linear viscoelasticity. However, another peculiar rheology prevails in such blends. Our preliminary experiments[11,13] revealed that the blends do not exhibit usual Newtonian flow behavior but exhibit a certain slow relaxation mechanism, i.e., some relaxation process with very long relaxation times. In this paper, the dynamic (linear viscoelastic) behavior of the blends of SB diblock copolymer and homopolybutadiene is examined in detail, and the molecular mechanism of slow relaxation is discussed in relation to the delayed motion of the entangled B blocks.

II. Experimental Section

Materials. Five SB diblock copolymer samples were prepared by an anionic polymerization method employing *sec*-butyllithium as the initiator and benzene as the solvent. The details of the synthesis were described elsewhere[10] and will not be repeated here. Table I shows the characteristics of these copolymers determined by a gel permeation chromatograph (GPC) equipped with a triple detector system consisting of a built-in refractometer, a UV-absorption detector, and a low-angle laser light scattering photometer connected in series.[10] The SB1 and SB2 were prepared from one

0024-9297/83/2216-0769$01.50/0

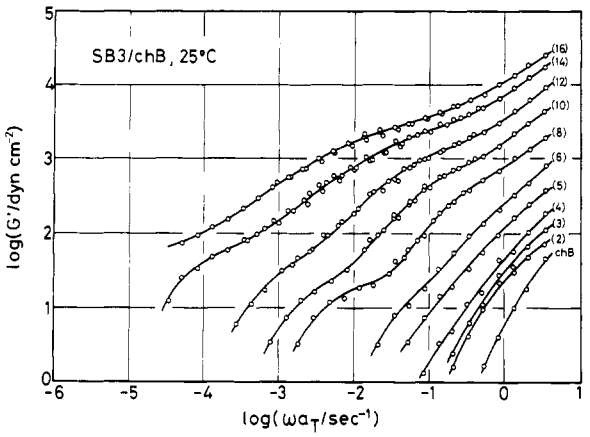

Figure 1. Master curves of the storage moduli G' of the SB3/chB blends reduced to 25 °C. The numerical values in the figure denote the content of SB3 in wt %.

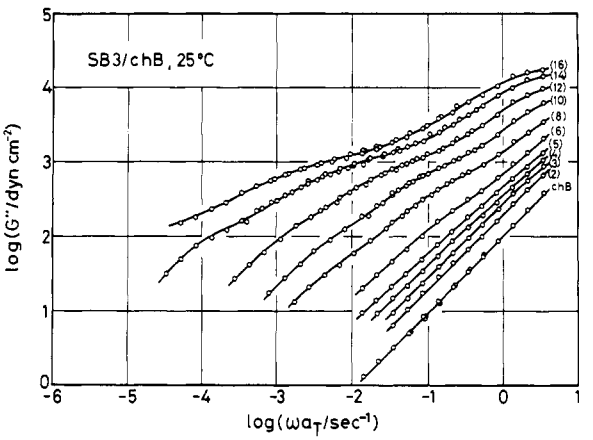

Figure 2. Master curves of the loss moduli G'' of the SB3/chB blends reduced to 25 °C. The numerical values in the figure denote the content of SB3 in wt %.

batch of living PS, and the SB3, SB4, and SB5 from another batch. Therefore, the S blocks of the SB1 and SB2 have the same characteristics and also those of the SB3, SB4, and SB5, as shown in Table I.

The systems examined were the blends of the copolymer and a commercially available homopolybutadiene (coded as chB; Nisseki PB 2000, Nihon Sekiyu Co.). The chB was used as received without further purification. The characteristics of the chB are also shown in Table I. The M_n of the chB is much lower than that of the B blocks of the SB samples, and the chB is completely miscible with the B matrix phase in the blends.[14]

To prepare a sample, we dissolved a prescribed amount of the SB, chB, and antioxidant, 2,6-di-*tert*-butyl-*p*-cresol (BHT) (about 1% to the blend), in a large excess of methylene chloride, which was subsequently evaporated to obtain a transparent blend.[2] The volume fraction of the B phase, in which the B blocks of the SB sample and chB molecules are contained, is much larger than that of the S phase. Therefore, micelles with spherical S cores and B cilia are formed in the blends.[15]

Rheological Measurements. Dynamic measurements were carried out with a conventional rheometer (an Autoviscometer L-III, Iwamoto Seisakusho, Kyoto) mounted with a cone-and-plate assembly. The radius of the cone was 15.0 mm and the angle between the cone and plate was 3.68°. The blends showed linear viscoelasticity as long as the content of SB was not extremely high (≲20%) and as long as the amplitude of the oscillatory strain was kept small (<0.3). The storage (G') and loss (G'') moduli were determined by the Markovitz equation.[16] The measurements were carried out at several temperatures. The time–temperature superposition principle[17] was applicable to those data. Since the blends contained a large number of carbon–carbon double bond of the B segments and were unstable at high temperatures, the measurements were carried out under a nitrogen gas atmosphere and the antioxidant BHT was added in the blends. However, the blends became yellow colored and oxidative degradation occurred within an hour at about 160 °C. Therefore, the measurements were made at temperatures below 160 °C. The frequency range was $0.1 < \omega/s^{-1} < 5$, where ω denotes the angular frequency. At the highest temperature chosen, most of the blends exhibited Newtonian behavior in the range of frequency examined.

III. Results and Discussion

1. Master Curves and Relaxation Spectra. Figures 1 and 2, respectively, show the master curves of the storage (G') and loss (G'') moduli for the SB3 blends reduced to 25 °C. The numerical values in the figures represent the content of the SB3 sample in wt %. For comparison, the behavior of the chB sample is also shown in the figure. The time–temperature superposition principle was approximately valid. Chung and Gale[18] reported that the mixing of the S and B blocks took place at about 170 °C in a bulk SBS triblock copolymer with a relatively low molecular weight of 7×10^3 (S)–43×10^3 (B)–7×10^3 (S). Our SB samples have larger molecular weight S and B blocks (see Table I) and the extent of intermixing of the S and B blocks seems to be small at temperatures <160 °C. As seen in Figures 1 and 2, the G' and G'' show a shoulder or plateau region when plotted against ω, when the content of the SB sample exceeds a certain value. This plateau region extended to a lower frequency region with increasing SB content. Although the figures are not shown here, similar results were obtained for the other SB/chB blends.

For many concentrated suspensions of small particles in polymeric media, a similar plateau often appears and is called the second plateau.[19–21] Onogi and co-workers[19–21] pointed out that the second plateau is indicative of the existence of a slow relaxation mechanism attributable to formation and dissociation of aggregates of the suspended particles. Such suspensions often show nonlinear dynamic behavior and pseudoplastic steady flow. However, our SB/chB blends do not contain aggregates of micelles and do exhibit linear viscoelasticity.[11] The plateau of the SB/chB blends must be attributed to a slow relaxation mechanism other than the aggregation and dissociation of the micelles. Kitamura and co-workers[22,23] examined a system consisting of cross-linked polybutadiene (PB) latices having grafted polystyrene (PS) cilia and suspended in polystyrene solution or melt. Their system showed linear viscoelasticity with a second plateau. The PB particles with PS grafts were randomly dispersed in the medium. In this aspect, their system is quite similar to our SB/chB blends. They attributed the origin of the second plateau to a local increase in the shear rate in the matrix phase between the surfaces of the neighboring suspended particles.[22,23] However, their idea seems to be inadequate for our SB/chB blends. The dimensions of their system are quite different from ours. Their PB particles have a radius of about 1300 Å and relatively short PS graft chains ($M \cong 50 \times 10^3$), while in our system the cores of the micelles have a radius as small as about 100 Å and are covered with the soft B block layer of average thickness about 200 Å or more (the molecular weight of the B block is varied from 46×10^3 to 262×10^3, as indicated in Table I).

The temperature dependence of the shift factor shown in Figure 3 is suggestive when we seek the origin of the second plateau in the SB/chB blends. The shift factor exhibits an Arrhenius-type activation process rather than a WLF-type behavior[17] for all the SB/chB blends and chB. Since almost all matrix B phases are occupied with the low molecular weight chB molecules, the fraction of the free

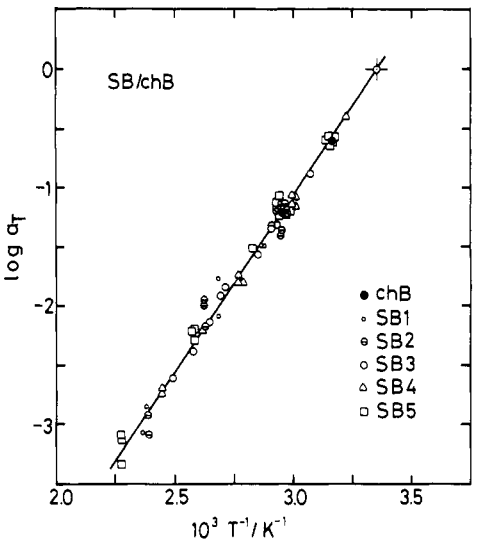

Figure 3. Arrhenius plots of the logarithm of the shift factor log a_T of the SB/chB blends and chB. The activation energy of flow for all systems is 14 kcal/mol.

Table II
Comparison of the Observed and Estimated Critical Concentrations of the SB/chB Blends

sample	obsd	estimated	
	c_R*/wt %	c_1*/wt %	c_2*/wt %
SB1/chB	6-8	5.3	10.1
SB2/chB	4-5	4.2	8.1
SB3/chB	5-6	3.9	7.4
SB4/chB	4-5	3.8	7.3
SB5/chB	3-4	3.1	6.0

volume and other microscopic properties may almost coincide with those of the chB, which shows an Arrhenius-type activation process and a Newtonian flow behavior with G' proportional to ω^2 and G'' to ω in this frequency and temperature range. The activation energy of flow ΔH_a is estimated for all the SB/chB blends and chB as $\Delta H_a \cong$ 14 kcal/mol. This result shows that the second plateau in the SB/chB blends may be attributed essentially to the retarded motion of the B blocks. It was pointed out that when one end of an entangled polymer chain is fixed in space, the motion of the entangled chain becomes strongly quenched or retarded.[24] The same mechanism appears to be operating in the SB/chB blends.

The idea for the origin of the second plateau in the SB/chB blends described above is also supported by the results shown in Figures 1 and 2. Namely, the SB/chB blends do not show a second plateau when the content of the SB is smaller than a certain critical value. Figure 4 shows the relaxation spectra H reduced to 25 °C for the SB1 to SB5 blends calculated from the G' and G'' master curves by using the Tschoegl approximation.[25] The numerical values in the figure represent the SB content in wt %. The spectra calculated from the master curves of G' and G'' coincided with each other within the error of the approximation. In the relaxation spectra H, we notice that the second plateau corresponding to a certain slow relaxation mechanism becomes apparent for the blends at a certain critical concentration. For example, a peak of the spectra appears between 6 and 8 wt % in the SB1/chB blend. The peak of the spectra extends to longer time as the content of the SB is further increased. Table II summarizes the rheologically observed critical concentration c_R* above which the second plateau appears. We estimated two critical concentrations, c_1* and c_2*, and compared these values with c_R*. c_1* is the average concentration at which

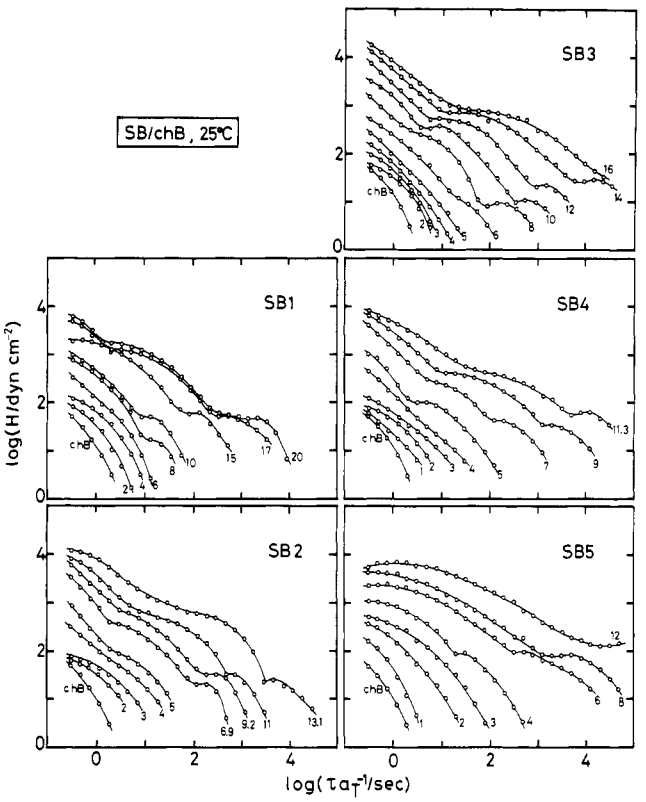

Figure 4. The relaxation spectra of the SB/chB blends reduced to 25 °C calculated from master curves of the dynamic moduli.

the micelles just begin to contact each other. On the other hand, c_2* is the concentration at which the segments of the B blocks begin to uniformly occupy the matrix B phase, i.e., the critical threshold. Both of the concentrations c_1* and c_2* are estimated as[10]

$$c_i^* = \left(\frac{100 f_i}{\rho}\right)\left(\frac{N_m M_{SB}}{(R_B + d_S)^3 N_A}\right) \qquad (i = 1, 2) \quad (1)$$

where N_m is the number of the SB molecules per one micelle, M_{SB} the molecular weight of the SB molecule, R_B the thickness of the B block layer d_S the radius of the S core, ρ the density of the system, and N_A the Avogadro number (cf. Figure 6). The numerical factor f_i is given, respectively, for i = 1 and 2 as

$$f_1 = 1/8 \qquad f_2 = 3/4\pi \qquad (2)$$

The structural parameters of the micelle, N_m and d_S, were already determined for n-tetradecane (C_{14}) solutions by a small-angle X-ray scattering (SAXS) study.[10] In the C_{14} solution, the micelles were arranged on a macrolattice and the scattering peaks due to the intermicellar and intramicellar interference could be resolved to determine N_m and d_S in the solution. However, no regular structure of the micelles was formed in the SB/chB blends and the higher order scattering peaks were not resolved in the blends.[11] Therefore, it is difficult to determine N_m and d_S directly from the SAXS data for the blends. However, when we compared the C_{14} solution and SB/chB blend having the same SB content, the position of the broad first-order scattering peak of the blend was almost the same as that of the first peak in the C_{14} solution.[11] This indicates that the nearest neighbor distance and the characteristics of the micelle (i.e., N_m and d_S) are almost the same in the C_{14} solution and in the blends. Thus, the values of N_m and d_S in the C_{14} solution[10] are used in the present estimation.

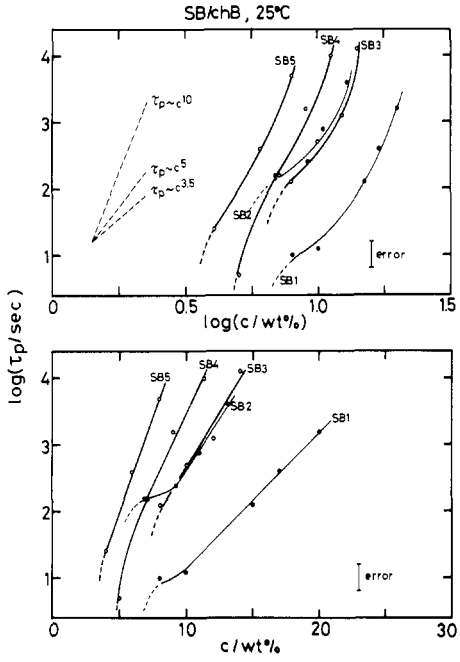

Figure 5. Concentration dependence of the longest relaxation time τ_p of the SB/chB blends reduced to 25 °C. The upper and lower row show the double-logarithmic and semilogarithmic plots of the concentration and τ_p, respectively. The broken lines in the upper row represent the power-law type dependences as indicated.

R_B can be estimated as the unperturbed end-to-end distance of the B block as[26]

$$R_B = bn_B^{1/2} \tag{3}$$

where b and n_B denote the Kuhn length and the degree of polymerization of the B block, respectively. The estimated results of c_1* and c_2* are also shown in Table II. As shown in the table, c_R* falls between c_1* and c_2*. This result indicates that the slow relaxation mechanism appears when the micelles begin to contact and overlap to some extent and the B blocks belonging to neighboring micelles become entangled with each other. The molecular weight of the chB is too small to generate any entanglements. Overlapping and entanglements of the micellar B blocks appear to be necessary to quench or retard the motion of the B blocks. The results of this comparison and the temperature dependence of the shift factor strongly suggest that the second plateau is due to the retarded motion of the entangled B blocks with its one end anchored on the stiff S cores.

2. The Longest Relaxation Time. We estimated the longest relaxation time τ_p from the peak of the relaxation spectrum in Figure 4 where the slowest relaxation mode appears. The dependence of the τ_p on the content c of the SB sample is examined in Figure 5. Figure 5 (top and bottom) shows double-logarithmic and semilogarithmic plots of τ_p against c, respectively. In Figure 5 (top), it should be noted that the dependence of τ_p on c cannot be described by a power-law form represented by the broken lines. Furthermore, the τ_p increases with c more rapidly than the power-law form of $\tau_p \propto c^{10}$. As shown in Figure 5 (bottom), the c dependence of τ_p is better approximated by an exponential relationship rather than by a power-law form. This dependence is quite different from that which appears in homopolymer systems. In solutions of linear homopolymers, the longest relaxation time τ_p, the plateau modulus G_N^0 or the steady-state recoverable compliance J_e^0, and the zero-shear viscosity η_0 show a power-law dependence on the concentration and molecular weight M as[27]

$$\eta_0 \sim c^5 M^{3.4} \tag{4a}$$

$$1/J_e^0 \sim G_N^0 \sim c^\alpha M^0 \tag{4b}$$

$$\tau_p \sim \eta_0/G_N^0 \sim c^{5-\alpha} M^{3.4} \tag{4c}$$

where α is a constant slightly larger than 2. The c dependence of τ_p of the SB/chB blends therefore contains an exponential enhancement. Such enhancement was already reported for star-shaped or branched homopolymers[27-31] and was concluded to be typical for the relaxation in a polymer chain with a fixed end. Graessley and co-workers[27-29] successfully reduced the concentration and molecular weight dependence of the zero-shear viscosity η_0 and the steady-state recoverable compliance J_e^0 of solutions of many star-shaped homopolymers. When the molecular weight of the star polymer increases, η_0 increases exponentially and J_e^0 increases proportionally to the molecular weight. These dependences are highly different from those of linear polymers shown in eq 4. However, in our SB/chB blends, the results shown in Figure 5 cannot be reduced in a universal curve in a manner similar to that applied for homopolymers, presumably because the concentration and molecular weight of the SB sample themselves are not suitable parameters for describing the motion of the anchored B blocks. To establish a universal curve for the τ_p of the SB/chB blends we employed the "tube" model[32-35] and sought suitable parameters describing the motion of the B blocks. For entangled linear homopolymer chains, the "tube" model provides an excellent picture relating the motion of the chain to its rheology and gives a satisfactory approximation for the power-law form of eq 4 especially for the zero-shear viscosity.[32] The "tube" model also predicts the results of a critical experiment, the stress relaxation after double-step strain.[33,36] On the other hand, for star-shaped homopolymer chains, Doi and Kuzuu[34] showed the appearance of an exponential enhancement factor and successfully simulated the experimental results of Graessley and Roovers.[28]

3. Analysis by the "Tube" Model. Figure 6 schematically shows the basic idea for describing the slow relaxation process, i.e., the reptational motion of an anchored B block in the SB/chB blends. As described earlier, chB molecules cannot form entanglements and are only considered as a uniform medium. When the content of the SB sample is increased beyond the critical value, the micelles overlap each other and the B cilia become entangled as shown in Figure 6a. When the extent of overlapping is not very large, only the segments near the free end seem to be trapped in the entanglements. The relaxation time τ_p of such a partially entangled cilium is estimated as follows. The entanglements near the free end of the cilium are replaced by a tube (Figure 6b) or slip links (Figure 6c). The free end of the cilium must diffuse back to the entrance of the tube near the core, on which the other end of the cilium is fixed, so that the cilium escapes from the tube confinement and relaxes. At that time, the end-to-end distance or, more precisely, the length of the projection of the cilium on the tube axis (contour length of the cilium measured along the tube axis) must become smaller than that at the equilibrium state. This process requires an extra (free) energy ΔU to shorten the chain length. According to Doi and Kuzuu,[34] this process is regarded as an activation process and the time τ_p required for such a process to take place is estimated as

$$\tau_p \cong \tau^{(1)} \exp(\Delta U/kT) \tag{5}$$

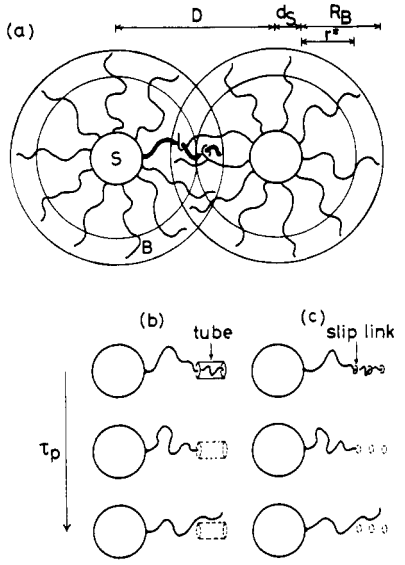

Figure 6. A schematic diagram indicating the entanglements of the B blocks with one end anchored on the S core. The symbols D, d_S, and R_B represent the mean distance between the centers of the neighboring micelles, the radius of the S core, and the thickness of the B block layer, respectively. As long as D is not too small, only the B segments near the free end are trapped in an entanglement network as shown in (a). This entanglement is replaced by (b) a tube or (c) slip links near the free end of the B block. The B block cannot pass across the tube or slip links. In the relaxation time τ_p of the B block, the free end of the B block must diffuse back to (b) the entrance of the tube near the S core or (c) the inner slip link so as to relax. The untrapped segments near the anchored end are approximated to occupy the spherical region with the radius of $r^* + d_S$.

where $\tau^{(1)}$ is the time required for a free chain with no fixed end to diffuse out from the tube.

To estimate the $\tau^{(1)}$ and ΔU, we approximated that the untrapped segments of the cilium occupy a spherical region of radius $r^* + d_S$, as shown in Figure 6a. The number of untrapped segments q is then estimated as

$$q \cong (r^*/b)^2 \tag{6}$$

The length of the tube L_t is estimated as

$$L_t \cong b\nu\frac{n_B - q}{n_e^{1/2}} \tag{7}$$

where n_e is the number of the segments between adjacent entanglement points and the ν is a numerical constant near unity. The equilibrium contour length of the cilium L_{eq} measured along the tube axis is now given as

$$L_{eq} \cong r^* + L_t = r^* + b\nu\frac{n_B - q}{n_e^{1/2}} \tag{8}$$

where the portion between the anchored end of the cilium and the entrance of the tube is regarded as another tube with much larger radius and length of r^*.

The increase in energy ΔU is estimated for a Gaussian chain as[34]

$$\Delta U \cong \frac{3}{2}kT\frac{(L_{eq} - r^*)^2}{n_B b^2} = \frac{3}{2}\nu^2 kT\frac{(n_B - q)^2}{n_B n_e} \tag{9}$$

On the other hand, the $\tau^{(1)}$ is estimated as

$$\tau^{(1)} \cong \frac{(L_{eq} - r^*)^2}{D_c} \cong \left(\frac{\zeta\nu^2 b^2}{kT}\right)\left(\frac{n_B(n_B - q)^2}{n_e}\right) \tag{10}$$

where D_c ($=kT/\zeta n_B$) is the diffusion constant of a chain consisting of n_B segments and ζ is the monomeric frictional constant.

From eq 5–10, the τ_p of the anchored B cilium is estimated as

$$\tau_p \cong \left(\frac{\zeta\nu^2 b^2}{kT}\right)\left(\frac{n_B(n_B - q)^2}{n_e}\right)\exp\left(\nu'\frac{(n_B - q)^2}{n_B n_e}\right) \tag{11a}$$

where ν' ($=^3/_2\nu^2$) is another constant. Equation 11a is rewritten in logarithmic form as

$$\ln \tau_p - \ln\left(\frac{n_B(n_B - q)^2}{n_e}\right) \cong \nu'\frac{(n_B - q)^2}{n_B n_e} + \ln\frac{\zeta\nu^2 b^2}{kT} \tag{11b}$$

where the symbol ln represents the natural logarithm.

To determine the number of segments between the adjacent entanglement points n_e, we must first determine r^*. For homogeneous homopolymer systems, n_e can be estimated from the plateau modulus or an integral of G'' with $\ln\omega$. However, in our SB/chB blends, the entangled region does not occupy the matrix phase uniformly and such an estimation is impossible. To estimate the r^*, we replaced the nonoverlapping regions by the spheres of radius $r^* + d_S$ just contacting each other. Then r^* is estimated as

$$r^* = (D/2) - d_S \tag{12}$$

where D is the mean distance between the centers of neighboring micelles as shown in Figure 6a. The value of D is simply estimated from the content c of the SB sample in the blend and the number N_m of SB molecules per micelle. From the values of D and r^*, the segment density ρ_e in the entangled region is estimated as

$$\rho_e = \frac{N_m(n_B - q)}{D^3 - (4\pi/3)(r^* + d_S)^3} \tag{13}$$

Then, from the value of ρ_e, the step length ξ_e of the primitive path in the entangled region is estimated as[35,37]

$$\xi_e \cong \xi^{bulk}(\rho^{bulk}/\rho_e)^{1/2} \tag{14}$$

where ξ^{bulk} and ρ^{bulk} represent the primitive-path step length and the segment density in the bulk homopolybutadiene. Doi[38] reported another scaling form of ξ_e and ρ_e. However, the value of ξ_e estimated according to Doi's equation[38] was too large. We employed eq 14 reported by Evans and Edwards[35] and de Gennes[37] and estimated the n_e as

$$n_e \cong (\xi_e/b)^2 = n_e^{bulk}(\rho^{bulk}/\rho_e) \tag{15}$$

Here n_e^{bulk} is the number of the segments between the adjacent entanglement points of the B blocks in the bulk state. A typical value of n_e^{bulk} for a polybutadiene synthesized by an anionic polymerization method (composition of the microstructure is cis:trans:vinyl = 43:50:7) is reported as[17]

$$n_e^{bulk} = 37 \tag{16}$$

The value of n_e^{bulk} shown in eq 16 is employed in our estimation, because our B blocks were synthesized by an anionic polymerization method.[10] The values of n_e and q are determined from eq 6 and 12–16. Figure 7 shows the relation of $\ln \tau_p - \ln (n_B(n_B - q)^2/n_e)$ vs. $(n_B - q)^2/n_B n_e$. Data for the blends with low SB content are eliminated in this figure because of the difficulty in estimating the parameters for such blends. All the results of the SB1 to SB5 blends are reduced in a universal curve, and this

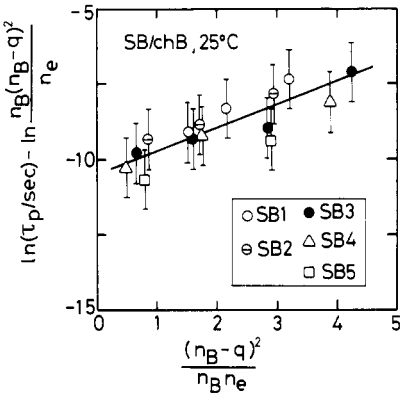

Figure 7. Plots of $\ln \tau_p - \ln (n_B(n_B - q)^2/n_e)$ vs. $(n_B - q)^2/(n_B n_e)$ of the SB/chB blends at 25 °C. The symbol ln represents the natural logarithm. The parameters q and n_e represent the number of untrapped segments per B block and the number of the segments between the adjacent entanglement points, respectively. n_B and τ_p are, on the other hand, the overall segment number of the B block and the longest relaxation time of the SB/chB blends, respectively.

universal relation coincides with that of the tube theory for partially entangled chain with a fixed end, eq 11. This result strongly suggests that the reptation of the B block anchored on the S core appears as the slow relaxation process in Figures 1 and 2.

In this connection, the slope ν' (=0.8) of the line in Figure 7 is close to the value of 0.66 employed by Doi and Kuzuu[34] in the simulation of the experimental results for star polymers.[28] In Figure 7, however, a strange result is also obtained. From the value of the intersect of the line, $\zeta\nu^2b^2/kT$ is estimated as 2.8×10^{-5} s. Employing the values of $b = 6.3 \times 10^{-8}$ cm, $\nu = 0.73$, and $kT = 4.11 \times 10^{-14}$ erg, we estimate the monomeric frictional constant as $\zeta = 5 \times 10^{-4}$ (dyn s)/cm. This value is about 10^5 times larger than the value, 4×10^{-9} (dyn s)/cm, reported for linear polybutadiene.[39] Since the value of ζ must be essentially the same in the SB/chB blends and in bulk polybutadiene, the discrepancy suggests that eq 5 must be slightly modified as

$$\tau_p \cong 10^5 \tau^{(1)} \exp(\Delta U/kT) \qquad (5')$$

A plausible explanation for this discrepancy is as follows: When the SB/chB blend undergoes stress relaxation, the B cilia escape from the "tube" confinement, and, at the same time, the spatial distribution of the micelles becomes the equilibrium one. A cooperative motion of the B cilia belonging to one micelle seems to be necessary when the latter process, i.e., the rearrangement of the micelle positions, takes place. Then the longest relaxation time τ_p of the SB/chB blend is expected to be much longer than the relaxation time $\tau^{(1)} \exp(\Delta U/kT)$ of a single cilium given in eq 5. The ratio of the relaxation times of the micelle rearrangement and the reptation of the single cilium must depend on the number of the cilia joining the cooperative motion, i.e., the number N_m of the SB molecules per micelle. All N_m of the SB1–SB5/chB blends are estimated to be ~90–100, and they do not change much.[10] If we assume that the ratio of the two relaxation times for the blends having almost the same N_m is always about 10^5 and independent of the SB content and micelle sizes, eq 5′ is derived. The validity of this assumption is not yet examined, and further theoretical study is desired.

Acknowledgment. This study is supported by the Ministry of Education, Science and Culture (Mombusho) under Grants 347081 and 543026, which are gratefully acknowledged.

Registry No. chB, 9003-17-2; SB, 9003-55-8.

References and Notes

(1) Kotaka, T.; White, J. L. *Trans. Soc. Rheol.* **1973**, *17*, 587.
(2) Masuda, T.; Matsumoto, Y.; Matsumoto, T.; Onogi, S. *Nihon Reoroji Gakkaishi* **1977**, *5*, 135. Masuda, T.; Matsumoto, Y.; Onogi, S. *J. Macromol. Sci., Phys.* **1980**, *B17*, 256.
(3) Osaki, K.; Kim, B. S.; Kurata, M. *Bull. Inst. Chem. Res., Kyoto Univ.* **1978**, *56*, 56.
(4) Watanabe, H.; Kotaka, T. *Nihon Reoroji Gakkaishi* **1980**, *8*, 26.
(5) Watanabe, H.; Kotaka, T.; Hashimoto, T.; Shibayama, M.; Kawai, H. *J. Rheol.* **1982**, *26*, 153.
(6) Kotaka, T.; Watanabe, H. *Nihon Reoroji Gakkaishi* **1982**, *10*, 24.
(7) Shibayama, M.; Hashimoto, T.; Kawai, H. *Macromolecules* **1983**, *16*, 16.
(8) Meier, D. J. *J. Polym. Sci., Part C* **1969**, *26*, 81; *Prepr. Polym. Colloq., Soc. Polym. Sci. Jpn.* **1977**, *1*, 83.
(9) Helfand, E.; Wasserman, Z. R. *Macromolecules* **1976**, *9*, 879; **1978**, *11*, 960.
(10) Watanabe, H.; Kotaka, T. *Polym. J.* **1982**, *14*, 739.
(11) Watanabe, H.; Kotaka, T. *J. Rheol.*, in press.
(12) Shibayama, M.; Hashimoto, T.; Kawai, H.; Watanabe, H.; Kotaka, T. *Macromolecules*, in press.
(13) Watanabe, H.; Yamao, S.; Kotaka, T. *Nihon Reoroji Gakkaishi* **1982**, *10*, 143.
(14) Kotaka, T.; Miki, T.; Arai, K. *J. Macrocmol. Sci., Phys.* **1980**, *B17*, 303.
(15) Sadron, C.; Gallot, B. *Macromol. Chem.* **1973**, *164*, 301.
(16) Markovitz, H. J. *Appl. Phys.* **1952**, *23*, 1070.
(17) See, for example: Ferry, J. D. "Viscoelastic Properties of Polymers"; Wiley: New York, 1969.
(18) Chung, C. I.; Gale, J. C. *J. Polym. Sci., Polym. Phys. Ed.* **1976**, *14*, 1149.
(19) Onogi, S.; Masuda, T.; Matsumoto, T. *Trans. Soc. Rheol.* **1970**, *14*, 275.
(20) Matsumoto, T.; Segawa, Y.; Warashina, Y.; Onogi, S. *Trans. Soc. Rheol.* **1973**, *17*, 47.
(21) Matsumoto, T.; Hitomi, C.; Onogi, S. *Trans. Soc. Rheol.* **1975**, *19*, 54.
(22) Masuda, T.; Kitamura, M.; Onogi, S. *Nihon Reoroji Gakkaishi* **1980**, *8*, 123.
(23) Kitamura, M.; Masuda, T.; Onogi, S. *Nihon Reoroji Gakkaishi* **1980**, *8*, 147.
(24) See, for example: de Gennes, P. G. "Scaling Concepts in Polymer Physics"; Cornell University Press: Ithaca, NY, 1979.
(25) Tschoegl, N. W. *Rheol. Acta* **1971**, *10*, 582.
(26) See, for example: Flory, P. J. "Statistical Mechanics of Chain Molecules"; Wiley: New York, 1968.
(27) Graessley, W. W.; Masuda, T.; Roovers, J. E. L.; Hadjichristidis, N. *Macromolecules* **1976**, *9*, 127.
(28) Graessley, W. W.; Roovers, J. E. L. *Macromolecules* **1979**, *12*, 959.
(29) Raju, V. R.; Menezes, E. V.; Marin, G.; Graessley, W. W.; Fetters, L. J. *Macromolecules* **1981**, *14*, 1668.
(30) Masuda, T.; Ohta, Y.; Onogi, S. *Macromolecules* **1971**, *4*, 763.
(31) Kajiura, H.; Ushiyama, Y.; Fujita, T.; Nagasawa, M. *Macromolecules* **1978**, *11*, 894.
(32) Doi, M.; Edwards, S. F. *J. Chem. Soc., Faraday Trans. 2* **1978**, *74*, 1789; **1978**, *74*, 1802; **1978**, *74*, 1818; **1979**, *75*, 38.
(33) Doi, M. *J. Polym. Sci., Polym. Phys. Ed.* **1980**, *18*, 1005; **1980**, *18*, 1981.
(34) Doi, M.; Kuzuu, N. *J. Polym. Sci., Polym. Lett. Ed.* **1980**, *18*, 775.
(35) Evans, K. E.; Edwards, S. F. *J. Chem. Soc., Faraday Trans. 2* **1981**, *77*, 1891; **1981**, *77*, 1913; **1981**, *77*, 1929.
(36) Fukuda, M.; Osaki, K.; Kurata, M. *J. Soc. Rheol., Jpn.* **1974**, *2*, 110.
(37) de Gennes, P. G. *J. Physiol. (Paris)* **1974**, *35*, 1133.
(38) Doi, M. *J. Phys. A: Math. Gen.* **1975**, *8*, 959.
(39) Estimated from the experimental data for the zero-shear viscosity and steady-state recoverable compliance reported by Graessley and co-workers.[29]